Analysis and Experiment of a Micro-Loss Multi-Port Hybrid DCCB for MVDC Distribution System

Weijie Wen, Bin Li, Botong Li, Haijin Liu, Jiawei He, Jiuxin Ma, and Ye Li

***Abstract*—Medium voltage direct current (MVdc) distribution system has numerous advantages over medium voltage alternative current distribution system. However, two shortcomings of the existing hybrid direct current circuit breaker (DCCB) with load current switch, including high construction cost and high operating losses, have constrained the application of existing hybrid DCCBs in MVdc distribution system. To overcome these two shortcomings, a novel multi-port hybrid DCCB with negative voltage source (NVS) has been proposed in this paper. First, the general topology and working principle of the multi-port hybrid DCCB with NVS are presented. Then, focused on the current commutation method and economic performance, comparisons between different hybrid DCCBs have been carried out. The analysis shows that by using multi-port hybrid DCCB with NVS, the construction cost could be reduced dramatically and the operating losses could be reduced to be comparable with alternative current circuit breaker, which are negligible. In the end, to fill the blank of experimental research, based on the topology of multi-port hybrid DCCB with NVS, a prototype with rating voltage of 2 kV has been established, and the test result have verified the multi-port hybrid DCCB with NVS.**

***Index Terms*—Current commutation, dc circuit breaker, failure mechanism, transient current interruption characteristics.**

I. Introduction

COMPARED with medium voltage alternative current (MVac) distribution system, voltage source converter (VSC)-based medium voltage direct current (MVdc) distribution system has the following features: enabling high penetration of renewable sources and energy storage elements, reducing power conversion stages, decreasing power losses, and operating costs. MVdc distribution system is getting more and more attraction [1]–[3].

Theoretically, there are mainly three approaches to deal with dc faults in MVdc distribution system.

1) Using alternative current circuit breaker (ACCB).
2) Using VSC with fault ride through capability [4], [5].

Manuscript received September 25, 2018; accepted November 5, 2018. Date of publication November 16, 2018; date of current version May 22, 2019. This work was supported in part by the China Postdoctoral Science Foundation under Grants 2017M621071 and 2018T110198, in part by the National Natural Science Foundation of China under Grants 51677126 and 51677095, and in part by the National Key Research and Development Program under Grant 2018YFB0904600. Recommended for publication by Associate Editor Z. Li. *(Corresponding author: Bin Li.)*

The authors are with the Key Laboratory of Smart Grid of Ministry of Education, Tianjin University, Tianjin 300072, China (e-mail:

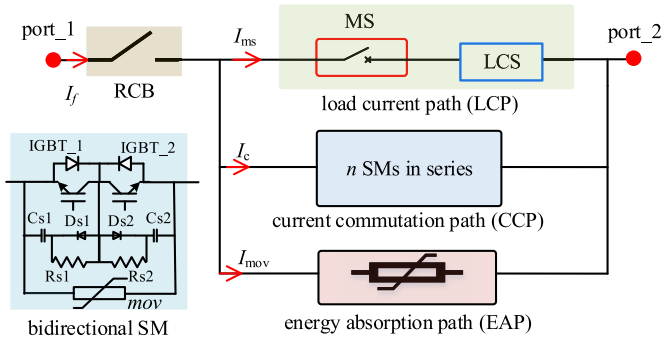

Fig. 1. Typical two-port hybrid DCCB proposed by ABB.

3) Using direct current circuit breakers (DCCBs).

The third approach appears to be the best [6], and many scholars have done impressive work on DCCB that has two ports (named as two-port DCCB in this paper) [7]–[16]. With advantages of high controllability and relative low operating losses, the two-port hybrid DCCB is regarded as one of the most promising solutions.

The typical two-port hybrid DCCB is proposed by ABB [8]–[10], and it is illustrated in Fig. 1. The typical two-port hybrid DCCB consists of a residual current breaker (RCB) in series with three parallel paths, including a load current path (LCP), a current commutation path (CCP), and an energy absorption path (EAP). RCB is an ultra-fast mechanical switch, and it is used to interrupt the residual current. LCP is composed of ultra-fast mechanical switch (MS) in series with a bidirectional load current switch (LCS). The bidirectional LCS is made of at least a submodule (SM) that is capable of interrupting bidirectional currents [9], [10]. CCP is made of *n* bidirectional SMs in series, and *n* is decided by the voltage level of the breaker. As shown in Fig. 1, each bidirectional SM proposed by ABB consists of two insulated gate bipolar transistor (IGBT), two RCD snubber circuit and a metal oxide varistor (*mov*) for protection. EAP is made of metal oxide varistor (MOV), and it is used for voltage limitation and energy absorption.

The working principle of the typical two-port hybrid DCCB [8]–[10] is described as follows.

1) *Normal state:* The current is completely conducted by RCB in series with LCP.
2) *Fault current interruption:* By turning OFF LCS, the fault current is commutated from LCP to CCP. Then, the transient interruption voltage (TIV) is established by turning OFF CCP. TIV is limited to be the clamping voltage of

EAP. Meanwhile, the fault current is commutated to EAP, and decreases gradually. After the residual energy in dc system is absorbed by EAP completely, a residual current flows through RCB in series with snubber circuits of CCP. Finally, the residual current is interrupted by RCB.

Because a two-port DCCB can only interrupt the fault current through a dc line, several two-port DCCBs should be installed on every dc node, and the number of two-port DCCBs on the node is equal to the number of the lines connecting with this node [17]. The number of nodes and lines in MVdc distribution system is much larger than high-voltage dc (HVdc) system at transmission level, meaning tens or even hundreds of two-port DCCBs are needed. In this case, the two following shortcomings will be amplified significantly.

A. High Construction Cost

By enquiring some reliable companies in China, such as Nanrui Co., Ltd, Pinggao Co., Ltd, and Xuji Co., Ltd, the price of a 10 kV two-port hybrid DCCB is 1 200 000–1 500 000 RMB and the price of a 10 kV ac circuit breaker (ACCB) is less than 50 000 RMB. Thus, a typical two-port hybrid DCCB is dozens of times more expensive than a ACCB with the same rating current and voltage. Observing the subassemblies of DCCB and ACCB, it is found that besides of MS (the main body of ACCB), SMs and MOV are used in the two-port hybrid DCCB, meaning that the construction cost of the two-port hybrid DCCB is mainly produced by the LCS, CCP, and EAP [18]–[21].

B. High Operating Losses, High Operating Cost, and Maintenance Difficulty Produced by LCS

ACCB is made of MS and its on-resistance is 20–60 $\mu\Omega$, meaning with load current of 1 kA, the operating losses are tens of watts, which are negligible. However, the operating losses, operating cost, and maintenance difficulty of the two-port hybrid DCCB are much higher than ACCB. The reason is described as follows. The current commutation from LCP to CCP is one of the prerequisites for successful current interruption. Although the arc voltage of MS (10–22 V) can drive the current commutation, considering that the arc voltage might not be large enough to ensure the fast and reliable current commutation [16], [22], LCS in the two-port hybrid DCCBs for MVdc distribution system should be reserved. As shown in Fig. 1, the load current would always flow through LCS (at least a IGBT in series with a diode), meaning that with load current of 1 kA, the operating losses could be ~2 kW, which is dozens of times higher than ACCB [9], [10], and the operating cost could be 20 000 RMB/year. To prevent excessive temperature rise, a reliable cooling system for LCS is essential, resulting in the maintenance difficulty.

Above all, both the construction cost and operating cost of DCCB in MVdc system is dozens of time higher than ACCB in MVac system. When tens or even hundreds of two-port hybrid DCCBs are used, the mentioned two shortcomings might result in the loss of economic advantage of MVdc distribution system over MVac distribution system.

Aimed to avoid the first shortcoming, multi-port hybrid DCCBs have been proposed based on the idea of sharing CCP and EAP [19]–[21]. Among these topologies, the one proposed in [21] appears to be the best, and it is shown in Fig. 2.

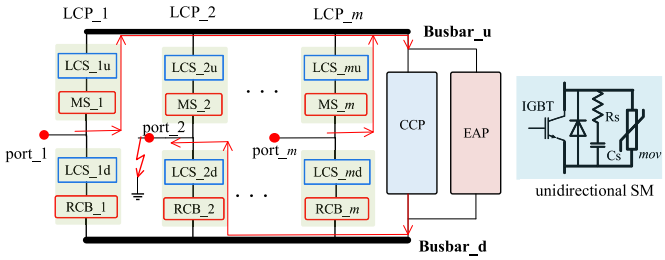

Fig. 2. Multi-port hybrid DCCB with LCS.

As shown in Fig. 2, by using multiple LCPs, a centralized CCP, and a centralized EAP, the multi-port hybrid DCCB could protect all the lines connecting with this breaker. In this way, the number of CCP and EAP in MVdc system could be reduced dramatically. Considering that CCP and EAP are the most expensive parts of a DCCB, the cost for the protection of MVdc system could be reduced significantly. However, the current commutation in the multi-port hybrid DCCB with LCS is ensured by configuring a unidirectional LCS on each bridge of LCP, and second shortcoming produced by LCS (high operating losses, high operating cost, and maintenance difficulty) is inevitable. In addition, the previous research works are focused on the simulation of multi-port hybrid DCCBs in dc system [19]–[21], and there is no relative experimental research. The emphasis of this paper is to eliminate the second shortcoming and to fill the blank of experimental research on multi-port hybrid DCCBs.

A novel multi-port hybrid DCCB with current commutated by a negative voltage source (NVS) is proposed in this paper, and its operating losses are comparable with ACCB (tens of Watts). For distinction, the novel DCCB is named as multi-port hybrid DCCB with NVS in this paper. The port number of multi-port hybrid DCCB with NVS (m) could be any integer greater than 1. The rest of this paper is organized as follows. The general topology and working principle of the multi-port hybrid breaker with NVS is presented in Section II. The comparison between the multi-port hybrid DCCB with NVS and the existing hybrid DCCBs is presented in Section III. Then, in Section IV, focused on multi-port hybrid DCCB with NVS itself, with m equal to 2, experimental research work have been carried out on a prototype developed in our Lab. In the end, Section V concludes this paper.

II. Multi-Port Hybrid DCCB With NVS

With m (port number) equal to 3, the general form of multi-port hybrid breaker with NVS and the cooperation of components in this breaker during the normal state and the current interruption process are presented in this part.

A. General Topology of Multi-Port Hybrid DCCB With NVS

Similar with MVac system, there are many nodes in MVdc distribution system. For the sake of comparison in Section III, taking the node that has three lines in Fig. 3 as an example, the

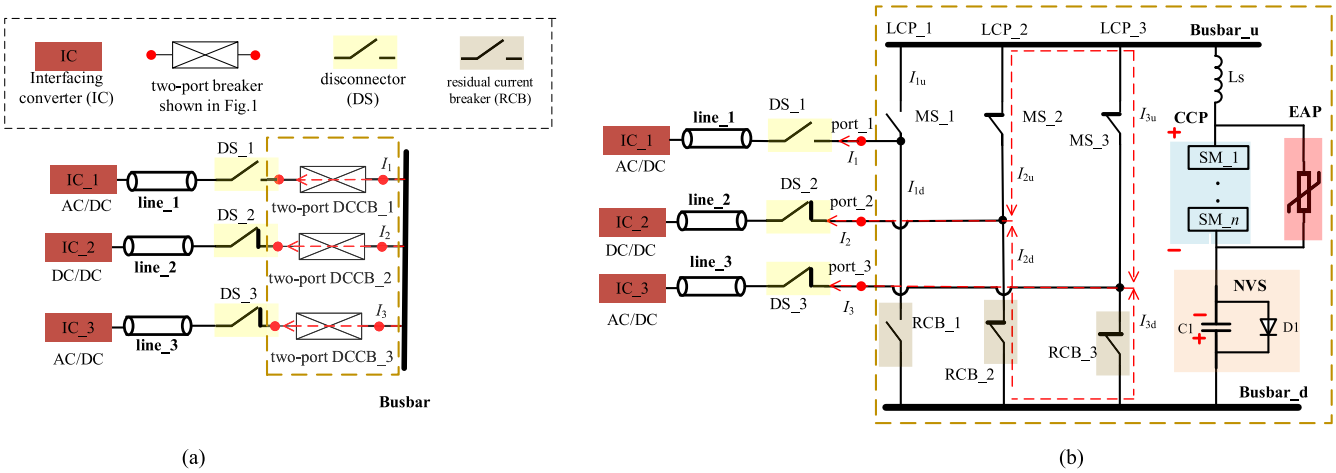

Fig. 3. Protection scheme based on different breakers at the node with 3 lines. (a) Protection scheme based on two-port hybrid breakers with LCS. (b) Protection scheme based on the three-port hybrid breaker with NVS.

protection scheme for this node, which is based on the typical two-port hybrid DCCB (see Fig. 1) and the three-port hybrid DCCB with NVS proposed by us are illustrated in Fig. 3(a) and (b), respectively.

In Fig. 3, IC_1 (ac/dc) is an interfacing converter between the MVdc system and the MVac system, and it is connecting with the node through line_1. IC_2 (dc/dc) is an interfacing converter between the MVdc system and the low voltage direct current (LVdc) loads or renewable sources, and it is connecting with the node through a line_2. IC_3 (ac/dc) is an interfacing converter between the MVdc system and the low voltage alternative current (LVac) loads or renewable sources, and it is connecting with the node through line_3. As shown in Fig. 3, besides of DCCB, a disconnector (DS) is installed on each line in case this line has to be isolated by this DS permanently.

In Fig. 3(a), the busbar of this node is named as Busbar and three typical two-port hybrid DCCBs (as shown in Fig. 1) are needed to protect all dc lines. As an alternative protection scheme, a three-port hybrid breaker with NVS is installed on the same node in Fig. 3(b). As shown in Fig. 3(b), there are two busbars at the same node, just like the two-busbar scheme in ac system. One is the up busbar (Busbar_u), and the other one is the down busbar (Busbar_d). The port is named as port_i (i = 1 – 3). IC_1 is connecting directly with port_1 through line_1. IC_2 is connecting with port_2 through line_2. IC_3 is connecting with port_3 through line_3. The general structure of three-port hybrid breaker with NVS is described as follows.

The three-port hybrid breaker with NVS consists of three LCP, a CCP, a EAP, and a NVS. load current path (LCP_i) is one-to-one connecting with dc line, and it is divided into an up bridge and a down bridge by port_i. The up bridge of LCP_i is composed of an ultra-fast MS (MS_i), and the down bridge of LCP_i is composed of RCB_i for the interruption of the residual current, just like RCB in Fig. 1.

Different from the bidirectional CCP in the typical two-port hybrid DCCB, the centralized current commutation path (CCP) in multi-port hybrid DCCB only need to interrupt unidirectional current (the reason will be explained in part C of this section), and it is made of n unidirectional SMs in series. The detailed diagram of unidirectional SM has been illustrated in Fig. 2. According to [23], injection enhanced gate transistor (IEGT) and integrated gate commutated thyristor could be an alternative of IGBT. In this paper, instead of IGBT, a IEGT with a monolithic integrated anti-parallel diode is used in the unidirectional SM. Besides, a RC snubber circuit and a *mov* are parallel with the IEGT in each SM for protection. Comparing the bidirectional SM in Fig. 1 and the unidirectional SM in Fig. 2, the device number in the unidirectional SM has been reduced by half, resulting in the cost of CCP in the multi-port hybrid DCCB is reduced by half.

EAP is the centralized energy absorption path made of MOV. It is used to limit TIV and to absorb the residual energy in MVdc system. It should be emphasized that the parameter of EAP, such as knee voltage, clamping voltage, and energy capacity, are consistent with that in the typical two-port hybrid DCCB.

NVS is a NVS that is first proposed in this paper, and it is made of a capacitor (C1) anti-paralleled with a diode (D1).

B. Normal State of Multi-Port Hybrid DCCB With NVS

During normal state, decided by the operation mode of MVdc system, dc lines of a common node could be divided into two groups. The first group (G1) is the collection of dc lines that do not conduct the load current; dc on these lines should be open, and mechanical switches in LCPs connecting with these lines should also be open, including MS on up bridge and RCB on down bridge. The second group (G2) is the collection of dc lines that should conduct the load current; DS on these dc lines should be closed, and mechanical switches in LCPs connecting with these lines are closed.

Taking the operation mode shown in Fig. 3 as an example, line_1 belongs to G1 and the other lines (line_2∼line_3) belong to G2. Therefore, DS_1, MS_1, and RCB_1 are kept open; DS_2∼DS_3, MS_2∼MS_3, and RCB_2∼RCB_3 are closed. The load current only flows through MS and RCB in LCP_2∼LCP_3. Because the on-resistance of MS and RCB is

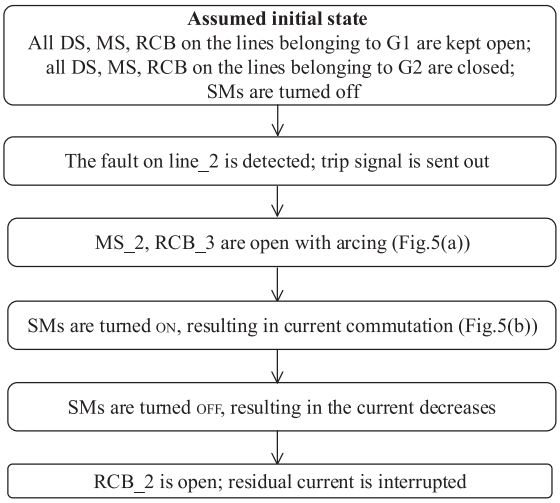

Fig. 4. Action sequence of components in the three-port hybrid DCCB with NVS when the fault occurs to line_2.

very small (20∼60 $\mu\Omega$), the operating losses of the three-port hybrid DCCB with NVS are comparable with ACCB (tens of watts) and the electric potential of Busbar_u is almost equal to Busbar_d.

During normal state, the turn-ON signal for IEGT in each unidirectional SM must be withdrawn, resulting in all SMs in CCP are turned OFF. The capacitor in NVS (C1) is pre-charged, and the direction of pre-charged voltage on NVS is shown in Fig. 3(b). The value of the pre-charged voltage should be designed properly, and hundreds of volts are enough for the 10 kV multi-port hybrid DCCB with NVS in MVdc distribution system. Because the electric potential of Busbar_u is almost equal to that of Busbar_d, the total voltage on the SMs in CCP is equal to the pre-charged voltage on NVS, and its direction is also shown in Fig. 3.

C. Current Interruption of Multi-Port Hybrid DCCB With NVS

The fault current is produced by the discharge of capacitors on the dc side of all interfacing converters (ICs), and it always flows out of the multi-port hybrid DCCB with NVS that should trip [21]. The multi-port hybrid DCCB with NVS is able to interrupt the fault current through any line that connects with the port of this breaker [19]–[21].

As mentioned in part B of this section, decided by operation mode of the system, the lines of a node are divided into two groups (G1 and G2). For the lines belonging to G1, no operation for DS, MS, and RCB is needed, and these mechanical switches are kept open during the whole current interruption process. In the lines belonging to G2, one is the fault line and the rest are the healthy lines. The mechanical switches on these lines belonging to G2 should cooperate with each other during the current interruption process.

Taking the fault occurring to line_2 shown in Fig. 3(b) as an example, the action sequence of components in the three-port hybrid DCCB with NVS is shown in Fig. 4 and the current path during the interruption process is illustrated in Fig. 5. The detailed cooperation of the mechanical switches on lines belonging to G2 is described as follows:

Before the fault, all DS, MS, and RCB of the lines belonging to G2 are closed and SMs are turned OFF.

Once the fault occurring to line_2 is detected, the MS on up bridge of LCP connecting with the fault line (MS_2) and RCBs on the down bridge of LCPs connecting with the healthy lines (RCB_3) are open with arcing, and the current path is shown in Fig. 5(a).

When contacts distance of these mechanical switches (MS_2, RCB_3) reaches 1∼2 mm, SMs of CCP are turned ON. Driven by NVS, the currents in all LCP start commutating to CCP in series with NVS until these mechanical switches (MS_2, RCB_3) are extinguished, resulting in the current commutation is finished and the current path after the current commutation is shown in Fig. 5(b).

Then, after the dielectric strength of these mechanical switches (MS_2, RCB_3) has recovered to be able to withstand TIV, SMs are turned OFF, resulting in the current is commutated from IEGTs to RC snubber circuits and then to EAP and TIV equal to clamping voltage of EAP is established. Because TIV (∼1.5 p.u.) is larger than the output voltage on dc side of all ICs in MVdc system, the current decreases gradually. Decided by the volt–ampere characteristic of EAP, TIV decreases with the decreasing of the current until the residual energy stored by the lines and inductors in MVdc system is absorbed completely, resulting in a residual current is commutated back to RC snubber circuits.

Finally, RCB on the down bridge of LCP connecting with the fault line (RCB_2) is open to interrupt the residual current.

After hundreds of milliseconds for the de-ionization of the short-circuit point, RCB on the down bridge of the fault line (RCB_2) is closed again. If no residual current is detected, the fault is temporary, and the MS on up bridge of LCP connecting with the fault line (MS_2) and RCBs on the down bridge of LCPs connecting with the healthy lines (RCB_3) are closed, resulting in that MVdc grids recover to the normal state, just as shown in Fig. 5(c). If a residual current is detected again, the fault is permanent. RCB on the down bridge of the fault line (RCB_2) is open again to interrupt the residual current. Then, DS_2 on the fault line is open to isolate the permanent fault, and RCBs on the down bridge of LCPs connecting with the healthy lines (RCB_3) are closed. As a result, the healthy area works continuously, just as shown in Fig. 5(d).

With different short-circuit point and initial state before the fault, the specific cooperation of components in multi-port hybrid DCCB with NVS is also different. However, no matter which line is faulty, based on the cooperation of the components, the fault current through CCP after commutation is unidirectional [21], and it can be interrupted by unidirectional SMs without arc. Thus, for dc nodes with m lines, a m-port hybrid DCCB with NVS could be used to replace m typical two-port hybrid DCCB with LCS.

III. Performance Discussion of Different Hybrid DCCB

This section is focused on the performance comparison between the existing hybrid DCCBs and the multi-port hybrid DCCB with NVS proposed in this paper. Considering that

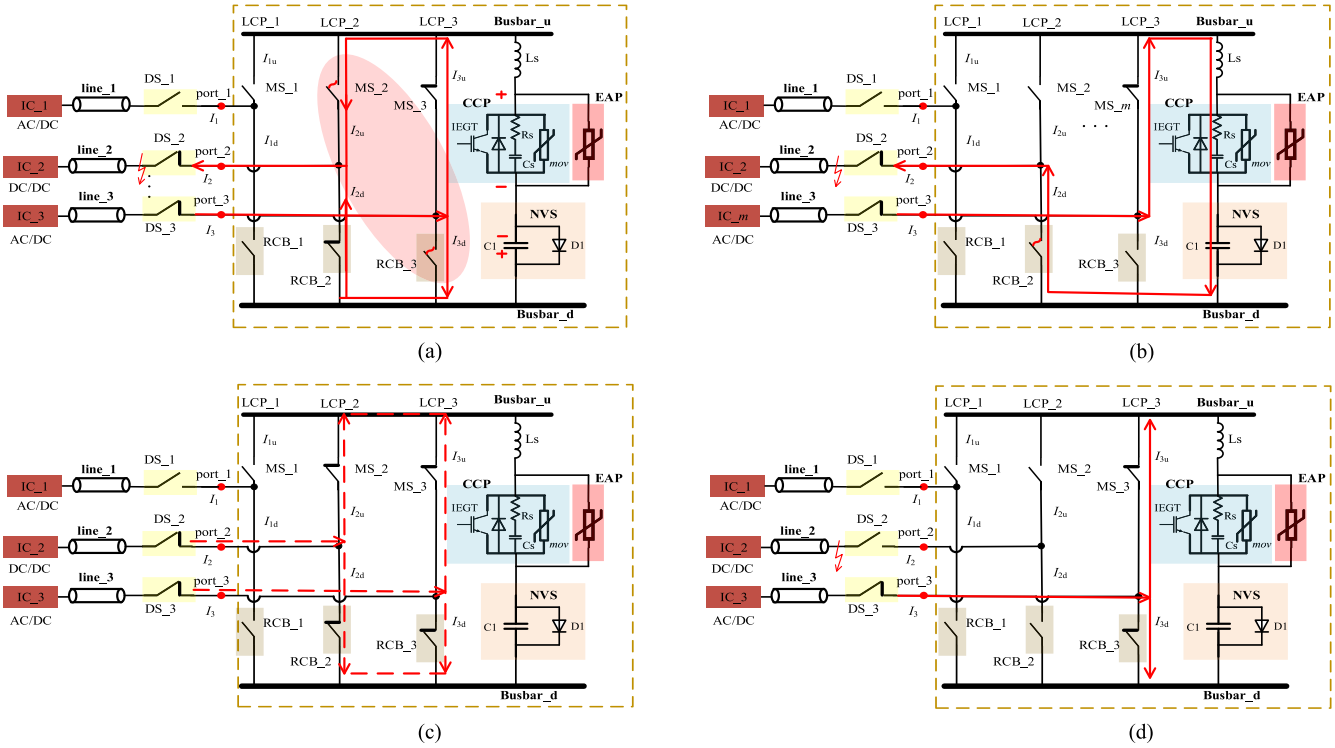

Fig. 5. Current path during the interruption process of three-port hybrid DCCB with NVS. (a) Before current commutation. (b) After current commutation. (c) After the isolation of a temporary fault. (d) After the isolation of a permanent fault.

the main differences are the current commutation method and the economic performance, these two aspects are discussed as follows.

A. Discussion on the Current Commutation Method

The current commutation from LCP to CCP is one of the prerequisites for successful current interruption. Taking the case in which the fault point is located near port_2 of the three-port hybrid DCCB as an example, the working principle of the current commutation method based on LCS and NVS is revealed, respectively.

The equivalent circuit of the three-port hybrid DCCB with LCS at the initial stage of the current commutation is illustrated in Fig. 6(a), and the equivalent circuit of the three-port hybrid DCCB with NVS at the initial stage of the current commutation is illustrated in Fig. 6(b). In Fig. 6, Ls_1u, Ls_1d, Ls_2u, Ls_2d, Ls_3u, Ls_3d, and Ls_CCP is the stray inductance of each path, and they are decided by the physical layout of the components. By designing the physical layout properly, the stray inductance of each bridge of LCS could be ensured to be equal.

In Fig. 3(b), once the fault occurs to line_2 at the outlet of port_2, the capacitors on dc side of IC_1 and IC_3 will discharge through the short-circuit point, and the real direction of the fault current through port_1, port_2, and port_3 is shown in Fig. 6. Before the current commutation, because the stray inductance in each bridge is equal, the current through each port

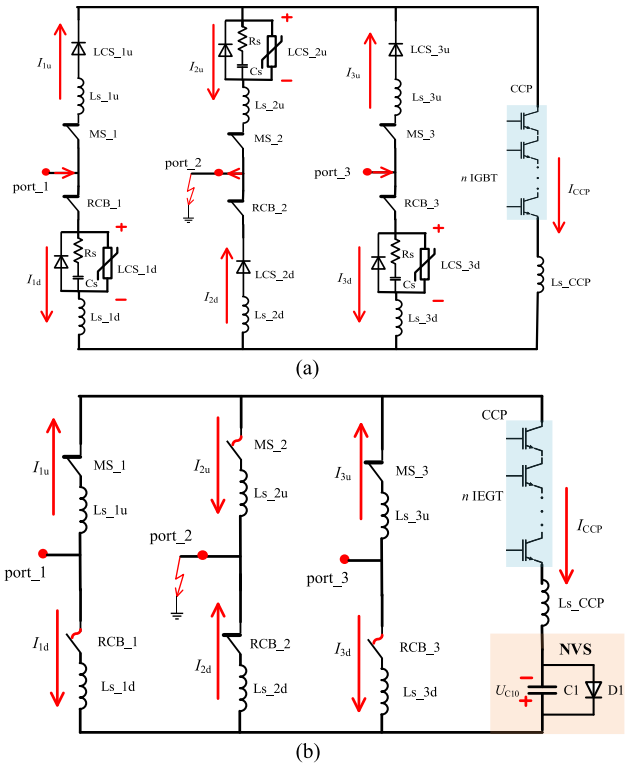

Fig. 6. Equivalent circuit of the three-port hybrid DCCB in the initial stage of current commutation process. (a) Equivalent circuit of the three-port hybrid DCCB with LCS. (b) Equivalent circuit of the three-port hybrid DCCB with NVS.

is almost equally divided into the up bridge and the down bridge ($I_{1u} = I_{1d}$; $I_{2u} = I_{2d}$; $I_{3u} = I_{3d}$).

According to the cooperation of the components in the three-port hybrid DCCB with LCS, once the fault occurs to line_2, LCS_1d, LCS_2u, and LCS_3d are turned OFF before RCB_1, MS_2, and RCB_3d are open. When LCS_1d, LCS_2u, and LCS_3d are turned OFF, they could be regarded as three parallel branches including a diode, a RC snubber circuit and a *mov*, just as shown in Fig. 6(a). Considering that the current in LCS_1u, LCS_2d, and LCS_3u flow through the diode in the unidirectional SM, so they could be regarded as a diode, just as shown in Fig. 6(a).

For the LCP connecting with the healthy line (LCP_1 and LCP_3), the current through the down bridge is commutated to the up bridge in series with CCP, meaning I_{1d} (I_{3d}) decreases with I_{1u} (I_{3u}) and $I_{\rm CCP}$ increasing. For the LCP connecting with the fault line (LCP_2), the current through the up bridge is commutated to CCP in series with the down bridge, meaning I_{2u} decreases with I_{2d} and $I_{\rm CCP}$ increasing. With all mechanical switches closed and their on-state resistance negligible, the state equation of the equivalent circuit shown in Fig. 6(a) is illustrated as follows:

$$\begin{aligned}
&U_{\rm LCS_1d} - U_{\rm LCS_1u} - U_{\rm CCP} = \\
&\quad -(L_{s_1u} + L_{s_1d} + L_{s_ccp})\frac{dI_{1d}}{dt} - L_{s_ccp}\left(\frac{dI_{2u}}{dt} + \frac{dI_{3d}}{dt}\right) \\
&U_{\rm LCS_2u} - U_{\rm LCS_2d} - U_{\rm CCP} = \\
&\quad -(L_{s_2u} + L_{s_2d} + L_{s_ccp})\frac{dI_{2u}}{dt} - L_{s_ccp}\left(\frac{dI_{1d}}{dt} + \frac{dI_{3d}}{dt}\right) \\
&U_{\rm LCS_3d} - U_{\rm LCS_3u} - U_{\rm CCP} = \\
&\quad -(L_{s_3u} + L_{s_3d} + L_{s_ccp})\frac{dI_{3d}}{dt} - L_{s_ccp}\left(\frac{dI_{1d}}{dt} + \frac{dI_{2u}}{dt}\right).
\end{aligned} \tag{1}$$

In (1), $U_{\rm LCS\_1d}$ is the voltage on LCS_1d; $U_{\rm LCS\_1u}$ is the voltage on LCS_1u; $U_{\rm LCS\_2d}$ is the voltage on LCS_2d; $U_{\rm LCS\_2u}$ is the voltage on LCS_2u; $U_{\rm LCS\_3d}$ is the voltage on LCS_3d; $U_{\rm LCS\_3u}$ is the voltage on LCS_3u. With LCS_1d, LCS_2u, and LCS_3d turned OFF and currents flowing through *mov* in each LCS, $U_{\rm LCS\_1d}$, $U_{\rm LCS\_2u}$, and $U_{\rm LCS\_3d}$ are equal to the clamping voltage of *mov* in each LCS. With currents flowing through the diode of LCS_1u, LCS_2d, and LCS_3u, $U_{\rm LCS\_1d}$, $U_{\rm LCS\_2u}$, and $U_{\rm LCS\_3d}$ are equal to the voltage drop of the diode in each LCS. With *n* IGBTs in series in CCP turned ON and the current flowing through *n* IGBTs, $U_{\rm CCP}$ is the voltage drop of *n* IGBTs in series

$$\begin{aligned}
&U_{\rm LCS_1d} - U_{\rm LCS_1u} - U_{\rm CCP} > 0 \\
&U_{\rm LCS_2u} - U_{\rm LCS_2d} - U_{\rm CCP} > 0 \\
&U_{\rm LCS_3d} - U_{\rm LCS_3u} - U_{\rm CCP} > 0.
\end{aligned} \tag{2}$$

As long as the relational expression shown in (2) is true, the current will commutate. The current commutating speed could be described by d*i*/d*t*. With $U_{\rm CCP}$, $U_{\rm LCS\_1u}$, $U_{\rm LCS\_2d}$, and $U_{\rm LCS\_3u}$ in the range of tens of volts and nearly constant, the larger the clamping voltage of LCS ($U_{\rm LCS\_1d}$, $U_{\rm LCS\_2u}$, $U_{\rm LCS\_3d}$) is, the faster the currents commutate, and the smaller the stray inductances are, the faster the currents commutate. When the current through the down bridge of the healthy lines (LCP_1 and LCP_3) and the up bridge of the fault line (LCP_2) has decreased to zero, the contacts of RCB_1, RCB_3, and MS_2 are separated without arcing. Then, after RCB_1, RCB_3, and MS_2 have recovered to be able to withstand TIV, IGBTs in CCP are turned OFF.

According to the cooperation of the components in the three-port hybrid DCCB with NVS that is introduced in Section II-C, once the fault occurs to line_2, the mechanical switches on the down bridge of LCP connecting with the healthy lines (LCP_1 and LCP_3) and on the up bridge of LCP connecting with the fault line (line_2) are commanded to be open first, meaning contacts of RCB_1, MS_2, and RCB_3d are separated with arcing first. Then, after the distance between the contacts of RCB_1, MS_2, and RCB_3d reaches 1–2 mm within a time delay of ∼1 ms that is caused by the overrun and contact inertia [24], IEGTs of each SM in CCP are turned ON. At this time, the state equation of the equivalent circuit shown in Fig. 6(b) is illustrated as follows:

$$\begin{aligned}
&U_{C1} + U_{\rm RCB_1} - U_{\rm CCP} = \\
&\quad -(L_{s_1u} + L_{s_1d} + L_{s_ccp})\frac{dI_{1d}}{dt} - L_{s_ccp}\left(\frac{dI_{2u}}{dt} + \frac{dI_{3d}}{dt}\right) \\
&U_{C1} + U_{\rm MS_2} - U_{\rm CCP} = \\
&\quad -(L_{s_2u} + L_{s_2d} + L_{s_ccp})\frac{dI_{2u}}{dt} - L_{s_ccp}\left(\frac{dI_{1d}}{dt} + \frac{dI_{3d}}{dt}\right) \\
&U_{C1} + U_{\rm RCB_3} - U_{\rm CCP} = \\
&\quad -(L_{s_3u} + L_{s_3d} + L_{s_ccp})\frac{dI_{3d}}{dt} - L_{s_ccp}\left(\frac{dI_{1d}}{dt} + \frac{dI_{2u}}{dt}\right)
\end{aligned}$$

$$U_{C1} + U_{C10} - \frac{1}{C1} = \iint\left(\frac{dI_{1d}}{dt} + \frac{dI_{2u}}{dt} + \frac{dI_{3d}}{dt}\right)dt. \tag{3}$$

In (3), U_{C1} is the voltage on C1 of NVS. $U_{\rm RCB\_1}$ is the arc voltage of RCB_1; $U_{\rm MS\_2}$ is the arc voltage of MS_2; $U_{\rm RCB\_3}$ is the arc voltage of RCB_3. When the ultra-fast vacuum switch is used, the arc voltage of these mechanical switches is in the range of 10–22 V. $U_{\rm CCP}$ is the voltage drop of CCP consisting of *n* IEGTs in series

$$\begin{aligned}
&U_{\rm C1} + U_{\rm RCB_1} - U_{\rm CCP} > 0 \\
&U_{\rm C1} + U_{\rm MS_2} - U_{\rm CCP} > 0 \\
&U_{\rm C1} + U_{\rm RCB_3} - U_{\rm CCP} > 0.
\end{aligned} \tag{4}$$

As long as the relational expression shown in (4) is true, the current commutation could last until these arcing mechanical switches, including RCB_1, MS_2, and RCB_3d, are extinguished at the current zero-crossing point. The reason is the dielectric recovery speed of the vacuum switch could be several kV/μs and the transient recovery voltage on these vacuum switch immediately after the current zero-crossing points is only hundreds of volts. Therefore, no restrikes will occur to these mechanical switches, including RCB_1, MS_2, and RCB_3d,

meaning these mechanical switches could be definitely extinguished at the zero-cross point [22]. With the arc voltage of ultra-fast mechanical switches and U_{CCP} in the range of tens of volts and nearly constant, the larger U_{C1} is, the faster the currents commutate and the smaller the stray inductances are, the faster the currents commutate. The current commutation is finished after RCB_1, MS_2, and RCB_3d are extinguished. Then, after these mechanical switches, including RCB_1, RCB_3, and MS_2, have recovered to be able to withstand TIV, IEGTs in CCP are turned OFF.

Above all, in the three-port hybrid DCCB with LCS, the current commutation is driven by the clamping voltage of *mov* in each LCP established by the turn OFF of unidirectional LCS. In the three-port hybrid DCCB with NVS, the current commutation is driven by the negative voltage on NVS that is in series with CCP. Therefore, with other parameters determined, by designing the clamping voltage of *mov* in the unidirectional LCS in the multi-port hybrid DCCB with LCS, and U_{C10} and C1 in multi-port hybrid DCCB with NVS properly, the current commutating speed in the two kinds of DCCB could be ensured the same.

Comparing these two current commutation methods, the advantages and disadvantages of the current commutation method based on NVS are described as follows. The disadvantage is that during the current commutation process, some mechanical switches have to be open with arcing. However, the dielectric strength of ultra-fast mechanical vacuum switches could recover very fast in several micro-seconds, therefore, this shortcoming is acceptable [22]. The main advantages are as follows.

1) With no load current flowing through IEGT or diode, the operating losses of multi-port hybrid DCCB could be reduced by dozens of time, and they are comparable with conventional ACCB (micro-losses).
2) No the cooling system is needed for NVS and the maintenance difficulty could be reduced.
3) Comparing with several LCS made of full controlled devices, it is obvious that the construction cost of one NVS made of conventional electric components, including a capacitor and a diode, is much lower [18].

B. Discussion on the Economic Performance

For a node with *m* lines in MVdc distribution system, there are three protection schemes. Protection scheme I is based on the typical two-port hybrid DCCB with LCS. Protection scheme II is based on the *m*-port hybrid DCCB with LCS. Protection scheme II is based on *m*-port hybrid DCCB with NVS. The specific numbers of the components used in the three protection schemes are listed in Table I.

In Table I, *m* is the number of the lines connecting with the node. *n* is the number of SM in CCP. With the maximum blocking voltage of IGBT (or IEGT) equal to ∼4.5 kV and the safety margin larger than 2, the permanent rating voltage of a SM is usually designed to be ∼2 kV, meaning *n* is equal to 5 in DCCBs for the MVdc distribution system of 10 kV [23]. In reference to the detailed diagram of bidirectional SM in Fig. 1 and unidirectional SM in Fig. 2, the IGBT (or IEGT) module in Table I consists of a IGBT, an anti-paralleled diode, a RC snubber circuit, a *mov*, a suit of power supply, and driver for IGBT (or IEGT) [23].

TABLE I
COMPARISON OF THE THREE PROTECTION SCHEMES

Item	Protection scheme I	Protection scheme II	Protection scheme III
Number of DS	*m*	*m*	*m*
Number of DCCB	*m*	1	1
Number of MS	*m*	*m*	*m*
Number of RCB	*m*	*m*	*m*
Number of EAP	***m***	**1**	**1**
Number of IGBT (or IEGT) module in CCP	**2·*m*·*n***	***n***	***n***
Number of IGBT (or IEGT) module in LCS	**2·*m***	**2·*m***	**0**
Number of NVS	**0**	**0**	**1**

As shown in Table I, the number of lines connecting with this node is *m* and a DS is needed for each line. Thus, the number of DS is equal to *m* in the three different protection schemes. For the node with *m* lines, *m* typical two-port hybrid DCCB with LCS are needed in protection scheme I; a *m*-port hybrid DCCB with LCS is needed in protection scheme II; a *m*-port hybrid DCCB with NVS is needed in protection scheme III.

In reference to the detailed topologies shown in Figs. 1–3, the total number of MS and RCB is *m* in the three protection schemes. Comparing with protection scheme I, the number of EAP is reduced from (*m*) to 1, and the number of IGBT (or IEGT) module in CCP is reduced from (2 *m*·*n*) to (*n*) in protection scheme II and III. For DCCBs with LCS, at least one SM is needed for each LCS to ensure the fast and reliable current commutation. Therefore, in protection scheme I and II, the number of IGBT (or IEGT) module in the LCS for current commutation is the same and it is equal to (2·*m*). In protection scheme III, a NVS is used to replace (2·*m*) unidirectional SM to ensure the current commutation.

As mentioned in Section I (the introduction part of this paper), the construction cost of DCCB is mainly produced by EAP and the IGBT (or IEGT) modules in CCP and LCS. Thus, comparing with protection scheme I, the construction cost of the protection scheme II and III based on multi-port hybrid DCCB is much lower and the larger *m* is, the more the construction cost could be reduced. Comparing protection scheme II and III, as presented in part A of this section, when a NVS is used to replace many LCS, the operating losses, the high operating cost, and maintenance difficulty produced by LCS could be eliminated in protection scheme III.

Above all, considering the construction cost, the operating losses, operating losses, and maintenance difficulty, protection scheme III based on the multi-port hybrid DCCB with NVS is the best. The larger *m* is, the more obvious the advantages of multi-port hybrid DCCB with NVS are. There are much more nodes and lines in MVdc distribution system than HVdc system

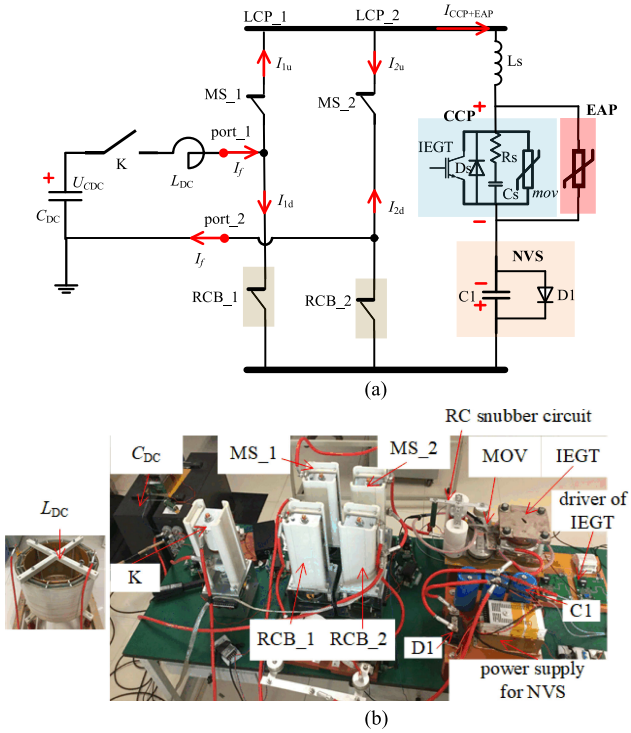

Fig. 7. Test circuit and pictures of the experiment platform and the prototype. (a) Test circuit for the prototype. (b) Picture of the experiment platform and the prototype.

at transmission level. Thus, the multi-port hybrid DCCB with NVS is quite suitable for the MVdc distribution system.

IV. Experiments on Multi-Port Hybrid DCCB With NVS

As mentioned earlier, the previous study on multi-port hybrid DCCB is focused on the simulation, and no experimental research has been carried out. In the simulation model and the theoretical analysis of the multi-port hybrid DCCB with NVS, it is assumed that the mechanical switches could be extinguished at the current zero-crossing point. To verify this assumption and the feasibility of the multi-port hybrid DCCB with NVS, based on the topology shown in Fig. 3(b), with m equal to 2 and n equal to 1, a prototype with rating voltage of 2 kV has been established in our laboratory.

In reference to the typical experimental circuits for hybrid DCCBs [9], [18], [25], the test circuit shown in Fig. 7(a) is designed. With $C_{\rm dc}$ and $L_{\rm dc}$ equal to 40 mF and 1 mH, when the pre-charged voltage on $C_{\rm dc}$ is 0.6 kV, a current with peak value of ∼2.6 kA and frequency of ∼25 Hz is produced to simulate the direct current to be interrupted. Based on this test circuit, current interruption tests have been carried out on the prototype. The picture of the experiment platform and the prototype is illustrated in Fig. 7(b).

The parameters of the prototype are listed as follows. Ls is ∼6 μH; number of IEGT module is 1; Rs is 0.3 Ω; Cs is 12 μH; knee voltage, clamping voltage, and energy capacity of EAP is 2 kV, 3 kV, and 20 MJ; C1 is 520 μH; the pre-charged voltage on C1 is 0.4 kV, and its direction is shown in Fig. 7(a).

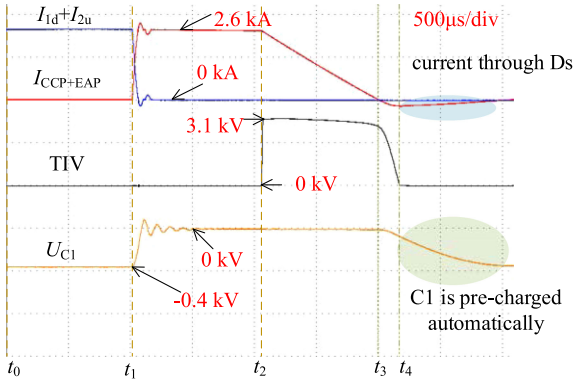

Fig. 8. Current interruption test result of the prototype.

As shown in Fig. 7(a), before the test, K (mechanical switch) is open, and the rest mechanical switches, including MS_1, MS_2, RCB_1, and RCB_2 are closed. $C_{\rm dc}$ and C1 are pre-charged. The test is ignited by the closing of K, and $C_{\rm dc}$ starts discharging through $L_{\rm dc}$, and the real direction of the current through each path has been marked in red in Fig. 7(a). The typical current interruption test result of the prototype is illustrated in Fig. 8.

In the test, with only two Rogowski coils, the currents through down bridge of LCP_1 and up bridge of LCP_2 are measured together as $(I_{1d}+I_{2u})$ in Fig. 8; the currents through CCP and EAP are measured together as $(I_{\rm CCP+EAP})$ in Fig. 8. With two differential probes, the voltage on CCP parallel with EAP is measured as TIV in Fig. 8; the voltage on C1 of NVS is measured as U_{C1} in Fig. 8.

As shown in Fig. 8, when the current reaches 2.6 kA, the contacts of MS_2 and RCB_1 are commanded to separate at t_0 (0 ms), and IEGT is triggered at t_1 (1 ms). After IEGT is turned on, driven by the negative voltage on C1 of NVS, the current commutation is characterized by that the currents through the down bridge on LCP_1 and the up bridge of LCP_2 $(I_{1d}+I_{2u})$ decreases with the current through CCP $(I_{\rm CCP+EAP})$ increasing. As shown in Fig. 8, the mechanical switches (MS_1 and RCB_1) are finally extinguished at the zero-crossing points, resulting in the current is completely commutated to CCP in series with NVS. With $(I_{\rm CCP+EAP})$ charging C1 continuously, along with an oscillation between C1 and L_S, U_{C1} increases from −0.4 kV until D1 starts conducting the current, resulting in U_{C1} equal to the voltage drop of D1 is ∼0 V. After a time delay for the dielectric recovery of the mechanical switches (MS_1 and RCB_1), IEGT is turned OFF at t_1 (2.1 ms), resulting in the current is commutated to RC snubber circuit and then to EAP, and TIV is limited to be clamping voltage of EAP (3.1 kV). Then, as shown in (5), with TIV larger than the voltage on $C_{\rm dc}$, $(I_{\rm CCP+EAP})$ starts decreasing

$$\frac{dI_{\rm CCP+EAP}}{dt}(L_{\rm DC}+L_s)={\rm TIV}-U_{\rm CDC}. \tag{5}$$

Decided by the volt-ampere characteristic of MOV in EAP, with $(I_{\rm CCP+EAP})$ decreasing, TIV also decreases slightly until it is lower than the knee voltage of MOV (2 kV) at t_3 (3 ms) and MOV in EAP recovers to the high impedance state. Then, CCP

parallel with EAP could be equivalent to the RC snubber circuit (Rs in series with Cs) parallel with diode (Ds) and TIV is equal to the voltage on Cs. Cs starts to discharge through C_{dc} and L_{dc}, resulting in TIV decreases further to zero until the residual current flows through Ds at t_4 (3.2 ms). The residual current is very small and it can be interrupted by opening RCB_2. In the end, after the current interruption, C1 is NVS can be recharged automatically to −0.4 kV by its power supply for the next operation.

Without losses of generality, based on topology proposed in this paper, a prototype with rating voltage of 2 kV was established. The test results have shown that a current of 2.6 kA could be interrupted by the prototype within 2.1 ms, and the multi-port hybrid DCCB with NVS has been verified by the experiments.

V. Conclusion and Prospects

In this paper, a novel multi-port hybrid DCCB with current commutated by NVS has been proposed to overcome the shortcomings of the existing hybrid DCCB with LCS, including the high construction cost and the high operating losses. The general topology of multi-port hybrid DCCB with NVS is presented and its working principle is theoretically analyzed. Then, in aspects of current commutation method and economic performance, comparisons between the existing hybrid DCCBs and the multi-port hybrid DCCB with NVS have been carried out. The analysis has shown that by using a multi-port hybrid DCCB, the construction cost could be reduced dramatically; by using the novel current commutation method based on NVS instead of LCS, the operating losses could be reduced to be comparable with ACCB, which are negligible and the operating cost and maintenance difficulty could be reduced dramatically. In the end, based on the topology of multi-port hybrid DCCB with NVS, a prototype with rating voltage of 2 kV has been established. The analysis of the test result has verified the multi-port hybrid DCCB with NVS. With features of low-construction cost and negligible operating losses, the multi-port hybrid DCCB with NVS is quite suitable for MVdc distribution system.

Future studies will be focused on the parameters optimization and the auto-closing function of multi-port hybrid DCCB with NVS.

References

[1] Y. Ji *et al.*, "Overall control scheme for VSC-based medium-voltage DC power distribution networks," *IET Gener. Trans. Distribution*, vol. 12, no. 6, pp. 1438–1445, Mar. 27, 2018.

[2] Y. Ji *et al.*, "Hierarchical control strategy for MVDC distribution network under large disturbance," *IET Gener. Trans. Distribution*, vol. 12, no. 11, pp. 2557–2565, Jun. 19, 2018.

[3] Z. Shuai, D. He, Z. Xiong, Z. Lei, and Z. J. Shen, "Comparative study of short-circuit fault characteristics for VSC-based DC distribution networks with different distributed generators," *IEEE J. Emerging Sel. Top. Power Electron.*, to be published, doi: 10.1109/JESTPE.2018.2834542.

[4] R. Zeng, L. Xu, L. Yao, and B. W. Williams, "Design and operation of a hybrid modular multilevel converter," *IEEE Trans. Power Electron.*, vol. 30, no. 3. pp. 1137–1146, Mar. 2015.

[5] J. Xu, P. Zhao, and C. Zhao, "Reliability analysis and redundancy configuration of MMC with hybrid submodule topologies," *IEEE Trans. Power Electron.*, vol. 31, no. 4, pp. 2720–2729, Apr. 2016, doi: 10.1109/TPEL.2015.2444877.

[6] Y. Wang, W. Wen, C. Zhang, Z. Chen, and C. Wang, "Reactor sizing criterion for the continuous operation of meshed HB-MMC-Based MTDC system under DC faults," *IEEE Trans. Ind. Appl.*, vol. 54, no. 5, pp. 5408–5416, Sep./Oct. 2018.

[7] X. Pei, O. Cwikowski, D. S. Vilchis-Rodriguez, M. Barnes, A. C. Smith, and R. Shuttleworth, "A review of technologies for MVDC circuit breakers," in *Proc. 42nd Annu. Conf. IEEE Ind. Electron. Soc.*, 2016, pp. 3799–3805.

[8] J. Häfner and B. Jacobson, "Proactive hybrid HVDC breakers—A key innovation for reliable HVDC grids," in *Proc. Cigré Symp.*, Bologna, Italy, 2011.

[9] A. Hassanpoor, J. Hafner, and B. Jacobson, "Technical assessment of load commutation switch in hybrid HVDC breaker," *IEEE Trans. Power Electron.*, vol. 30, no. 10, pp. 5393–5400, Oct. 2015.

[10] O. Cwikowski, M. Barnes, R. Shuttleworth, and B. Chang, "Analysis and simulation of the proactive hybrid circuit breaker," in *Proc. IEEE 11th Int. Conf. Power Electron. Drive Syst.*, Sydney, NSW, Australia, 2015, pp. 4–11.

[11] K. A. Corzine, "A new-coupled-inductor circuit breaker for DC applications," *IEEE Trans. Power Electron.*, vol. 32, no. 2, pp. 1411–1418, Feb. 2017.

[12] D. Keshavarzi, T. Ghanbari, and E. Farjah, "A Z-source based bidirectional dc circuit breaker with fault current limitation and interruption capabilities," *IEEE Trans. Power Electron.*, vol. 32, no. 9, pp. 6813–6822, Sep. 2017.

[13] A. Maqsood, A. Overstreet, and K. A. Corzine, "Modified Z-source DC circuit breaker topologies," *IEEE Trans. Power Electron.*, vol. 31, no. 10, pp. 7394–7403, Oct. 2016.

[14] A. Mokhberdoran, A. Carvalho, N. Silva, H. Leite, and A. Carrapatoso, "A new topology of fast solid-state HVDC circuit breaker for offshore wind integration applications," in *Proc. 17th Eur. Conf. Power Electron. Appl.*, Sep. 2015, pp. 1–10.

[15] W. Xiangguang, G. Chong, L. Xiang, Z. Wandi, and Wu Yanan, "A Novel design of high-voltage DC circuit breaker in HVDC flexible transmission grid," *Automat. Electr. Power Syst.*, vol. 37, no. 15, pp. 95–102, 2013.

[16] J. M. Meyer and A. Rufer, "A DC hybrid circuit breaker with ultra-fast contact opening and integrated gate-commutated thyristors (IGCTs)," *IEEE Trans. Power Del.*, vol. 21, no. 2, pp. 646–651, Apr. 2006.

[17] C. M. Franck, "HVDC circuit breakers: A review identifying future research needs," *IEEE Trans. Power Del.*, vol. 26, no. 2, pp. 998–1007, Apr. 2011.

[18] W. Wen, Y. Huang, B. Li, Y. Wang, and T. Cheng, "Technical assessment of hybrid DCCB with improved current commutation drive circuit," *IEEE Trans. Ind. Appl.*, vol. 54, no. 5, pp. 5456–5464, Sep./Oct. 2018.

[19] A. Mokhberdoran, D. Van Hertem, N. Silva, H. Leite, and A. Carvalho, "Multi-port hybrid HVDC circuit breaker," *IEEE Trans. Ind. Electron.*, vol. 65, no. 1, pp. 309–320, Jan. 2018

[20] G. Liu, F. Xu, Z. Xu, Z. Zhang, and G. Tang, "Assembly HVDC breaker for HVDC grids with modular multilevel converters," *IEEE Trans. Power Electron.*, vol. 32, no. 2, pp. 931–941, Feb. 2017.

[21] E. Kontos, T. Schultz, L. Mackay, L. M. Ramirez-Elizondo, C. M. Franck, and P. Bauer, "Multiline breaker for HVdc applications," *IEEE Trans. Power Del.*, vol. 33, no. 3, pp. 1469–1478, Jun. 2018.

[22] W. Wen, Y. Huang, Y. Sun, J. Wu, M. Al-Dweikat, and W. Liu, "Research on current commutation measures for hybrid DC circuit breakers," *IEEE Trans. Power Del.*, vol. 31, no. 4, pp. 1456–1463, Aug. 2016.

[23] Z. Chen *et al.*, "Analysis and experiments for IGBT, IEGT, and IGCT in hybrid DC circuit breaker," *IEEE Trans. Ind. Electron.*, vol. 65, no. 4, pp. 2883–2892, Apr. 2018.

[24] W. Wen *et al.*, "Research on operating mechanism for Ultra-Fast 40.5-kV vacuum switches," *IEEE Trans. Power Del.*, vol. 30, no. 6, pp. 2553–2560, Dec. 2015.

[25] W. Grieshaber *et al.*, "Development and test of a 120 kV direct current circuit breaker," in *Proc. Cigré*, Paris, France, 2014, Paper B4–301.

Authors' photographs and biographies not available at the time of publication.